PAPER • OPEN ACCESS

Investigation of the mechanism for current induced network failure for spray deposited silver nanowires

View the article online for updates and enhancements.

IOP ebooks™

Bringing you innovative digital publishing with leading voices to create your essential collection of books in STEM research.

Start exploring the collection - download the first chapter of every title for free.

Investigation of the mechanism for current induced network failure for spray deposited silver nanowires

D Fantanas[1,2,4] , A Brunton[2], S J Henley[2] and R A Dorey[3]

[1] EPSRC CDT in MiNMaT, University of Surrey, Guildford GU2 7XH, United Kingdom
[2] M-Solv Ltd, Oxonian Park, Kidlington OX5 1FP, United Kingdom
[3] Centre for Engineering Materials, University of Surrey, Guildford GU2 7XH, United Kingdom

E-mail: d.fantanas@surrey.ac.uk

Abstract

Silver nanowires are one of the prominent candidates for the replacement of the incumbent indium tin oxide in thin and flexible electronics applications. Their main drawback is their inferior electrical robustness. Here, the mechanism of the short duration direct current induced failure in large networks is investigated by current stress tests and by examining the morphology of failures. It is found that the failures are due to the heating of the film and they initiate at the nanowire junctions, indicating that the main failure mechanism is based on the Joule heating of the junctions. This failure mechanism is different than what has been seen in literature for single nanowires and sparse networks. In addition, finite element heating simulations are performed to support the findings. Finally, we suggest ways of improving these films, in order to make them more suitable for device applications.

Keywords: Rayleigh instability, Joule heating, electrical failure, nanowires, silver, transparent conductors, simulation

(Some figures may appear in colour only in the online journal)

1. Introduction

Transparent conductive coatings are highly sought after because of their many applications in state of the art electronic devices. The most common amongst these are: light emitting diodes (TVs, monitors, mobile phones), touch sensors (tables, mobile phones and laptops) and photovoltaics. Currently the industry-standard material for these applications is indium-doped tin oxide (ITO). But due to its high cost [1, 2], brittleness [3, 4] and non-reel-to-reel compatible deposition techniques [5, 6], alternatives are being heavily researched. Common ITO-free transparent conductors include metal-based nanomaterials, graphene,

carbon nanotubes, polymers, other oxides and hybrids of these. Some materials are more transparent or more conductive than others, making them more favorable for different applications. An example of this is touch sensors, where the transparency of the material in the visible range is vital. Furthermore, lower cost, reel-to-reel compatible and vacuum-free deposition techniques are required for use on flexible substrates and to further reduce the final device cost.

Silver nanowire (AgNW) based transparent conductors are currently one of the most promising materials to replace ITO in specific display and sensor applications, where low weight or flexibility are required. Recent developments in the production techniques have produced higher aspect ratio metal nanowires, which are more desirable for transparent conductors because in order to form a conductive network fewer nanowires are needed, which increases the film's optical transmission, while keeping the sheet resistance of the film low [7, 8]. Using filtration and other techniques, the dispersions of nanowires of similar thickness and length can

[4] Author to whom any correspondence should be addressed.

be produced. This makes the fabrication of uniform films feasible. Silver based nanowires exhibit high conductivity to optical transparency ratios. Silver nanowires have transmission in the visible range comparable to ITO and superior transmission in the rest of the spectrum for films of the same sheet resistance. Furthermore, the conductivity of these nanowires is superior making them more favorable for applications that need low resistance transparent materials. One of the main reasons that is hindering the industry from moving towards nanowires is their thermal, environmental and electrical instability [9]. Regarding the electrical instability, this can be broken down into two regimes. Firstly, AgNW have been shown to have low thresholds for electrostatic discharge damage, which is an important factor for incorporation of materials in consumer and industrial electronic devices. Secondly, there is considerable interest in using low cost flexible AgNW coatings as current collectors or heating panels, where their stability to sustained (DC/AC) current load is important. To date there has been little investigation of this second category, and mainly limited to investigations of individual nanowires, rather than networks.

It has been shown by Liu *et al* that the current carrying ability of nanowires is diameter dependent, with a peak at 34 nm [10]. Failures due to the electromigration in silver nanowires can occur at lower current densities also. Khaligh *et al* showed that nanowires form hillocks and then fail due to breakage at lower than maximum current densities, if the current is applied for long periods [6]. In their tests they applied a current density of 17 mA cm^{-2} across a 12 Ω/sq silver nanowire electrode for 17 days. This shows that electromigration is taking place even at lower current densities, with effects taking longer to manifest. Furthermore, for single nanowires, it has been shown that silver based nanomaterials fracture and alter their form with heat [11]. This occurs due to the high surface energy of the 110-crystallographic planes exposed, which are not the planes with the lowest energy in an FCC material [12]. Hence, the kinetic limitations to reconstruction can be overcome at only modest elevated temperatures. It should be noted that the majority of these studies have focused on individual wires and have not addressed realistic usages in large, dense networks. In order to understand this failure in realistic dense nanowire networks, tests on various samples at different nanowire densities and hence sheet resistances, were evaluated.

In a complementary work, Khaligh *et al*, discuss the failure of nanowire networks after long current exposure (multiple days) [13]. In this work we discuss the effect of high current densities over shorter period of times (seconds), more akin to the switching behavior in operating electrical circuits. Their results are more relevant to electromigration and oxidation of nanowires, whereas here the rapid failure due to localized heating is dominant.

2. Experimental Methods

The nanowires are commercially available, and their deposition was done by spraying, using a custom made automated spray system manufactured by M-Solv Ltd. The nanowire dispersions were diluted with isopropanol at various loadings depending on the material. The nanowires were sourced from two different suppliers, with dimensions of 15 and 30 nm from the first supplier and 40 nm from the second. For the spray deposition a Harder & Steenbeck XL2000 Airbrush with a 0.4 mm nozzle was used. The nanowire films were deposited at various densities on glass microscope slides. The microscope slides were cleaned with IPA and any dust particulates were removed using compressed air. The spray system is equipped with HEPA 17 filters to prevent particulates from being introduced on the sample surface. After deposition and when the nanowires are not being tested, they are stored in an inert atmosphere glove box to prevent the nanowires from being affected by heat, oxygen, moisture or light. Then test electrode structures, with the layout presented in figure 1(a), were formed by laser ablation, using an IR laser (1064 nm, 10 ns pulses). Silver paste was applied to both end electrodes to make electrical contact to the nanowire film in the middle area between them. The size of the nanowire test area was 20 × 20 mm. A Keithley 2420 source meter was used as a current source, under voltage control, to apply increasing voltages until the nanowire films failed. The voltage was stepped from 0 to 62 V, with the current limited to a maximum of 3A. The process was automated using a LabVIEW based program. Each voltage was applied for 1 s and the sample was left to cool down at zero volts between the increasing steps for 5 s. All the tests were conducted in the same temperature and humidity-controlled laboratory area as the spray deposition. The temperature was 20 °C and the relative humidity 35%. After failure, the damaged areas examined using a scanning electron microscope (SEM) in order to determine the nature of the failure.

3. Results and discussion

Figures 1(a)–(c) show SEM overview micrographs of the current induced failure of the nanowire films of different initial sheet resistances. The failure region can be seen as a bright line across the image. The failures can be seen as very bright white areas in the SEM, due to localized is charging, due to loss of conductivity. The nanowires failed perpendicularly to the current flow as can be seen in figures 1(b) and (d). It is suggested that this is happening due to the initial film failure originating from a weak point of the sample. This weak spot could be an area where there is a less dense patch of nanowires, and the local current density is higher. Such patches could be a result of the randomness of the spray deposition process or simply due to the stochastic nature of film assembly from extended 1D objects. As the current is driven from top to bottom in the schematic, when one area fails, a higher current density would need to pass either side of the defect along an axis perpendicular to the current flow. Such higher current densities would likely lead to further failures, resulting in sequential failing of neighboring nanowires and a rapid increase in resistance. This rapid chain reaction is likely why the resistance of the film suddenly increases, where the current plummets.
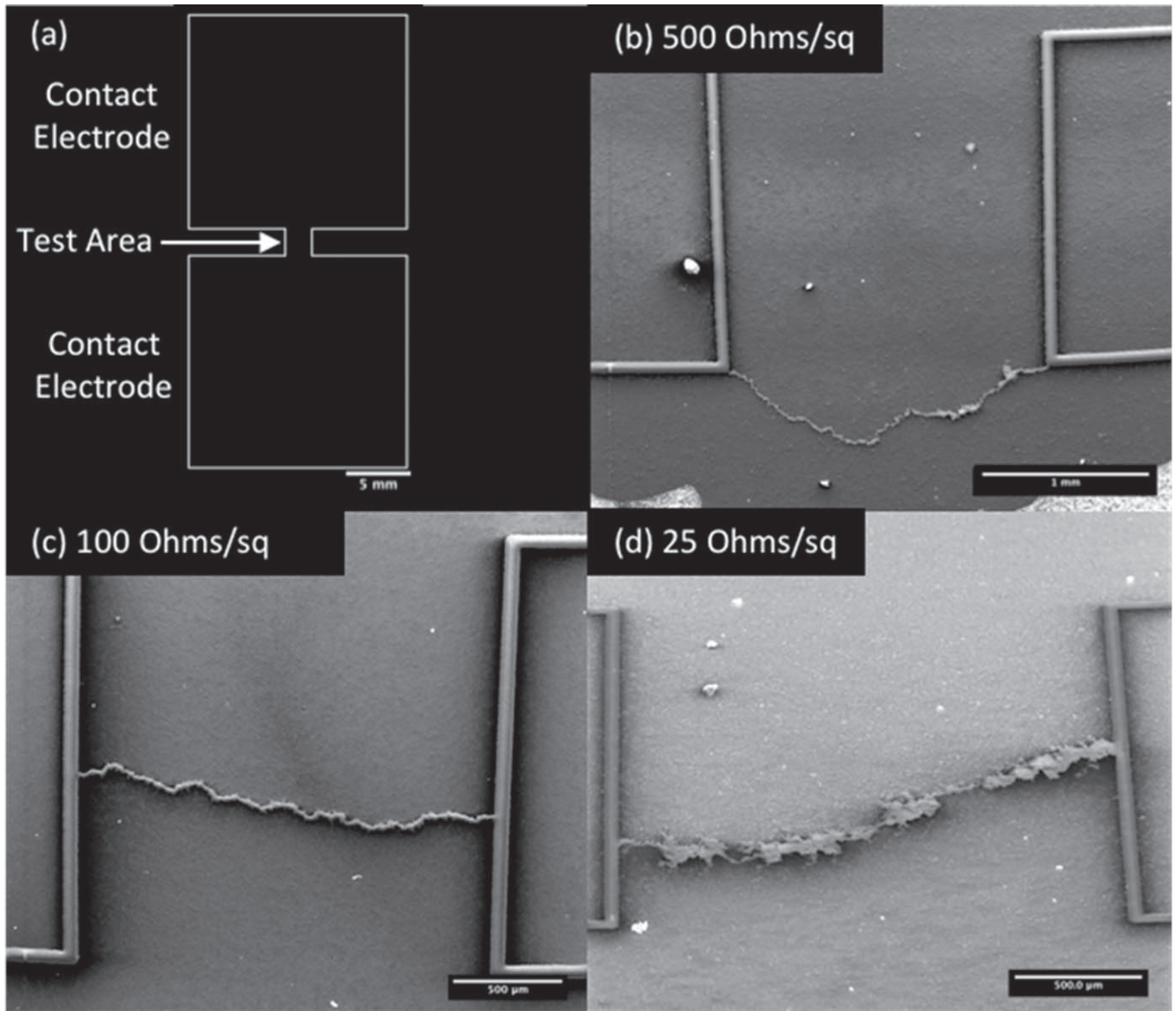
Figure 1. (a) Schematic of the test electrodes produced using IR laser ablation. (b)–(d) are SEM micrographs of the current induced failure of the nanowire films of 500, 100 and 25 Ohms/sq sheet resistances respectively.

From SEM micrographs of the AgNW from within these failed regions, as shown in figure 2, two different nanowire failure mechanisms have been identified, both resulting from Joule heating. The first one is the break of the nanowires with droplets of melted silver at the edges of the break (figures 2(a) and (c)). These failures initiate at the junctions, where the temperature is the highest. This occurs due to the Joule heating at the junctions. The temperatures here are higher, due to the higher contact resistance. Examples of this type of failure can be seen in figures 2(a) and (c). Not the whole length of the nanowires is 'melted', just at a certain point along its length. Once broken current stops passing through it, and the source of heating at this location ends. This has been identified in publications as incomplete failure of nanowires, where a hillock has been formed [10]. This type of failure has been observed in all the samples here, with sheet resistance not being a factor. The nanoparticles are created from the melting of the nanowires and cannot be seen in pristine samples (figure 3 left).

The second type of failure was observed in more conductive samples (below $250\,\Omega/\text{sq}$) with higher densities of nanowires. The nanowires break up in multiple droplets, as can be seen in figures 2(b) and (d). As can be observed, the mass transport that occurs during electromigration can result in the breaking of the nanowires into multiple spherical drops, due to the capillary or Rayleigh instability (figure 2(d)). When perturbation with wavelengths larger than $2\pi R_0$ (where R_0 is the radius of the cylinder) would result in the transformation of the cylinder into multiple spheres at equal distances and the mass is conserved. For different temperatures different results are expected, ranging from a single crack on the wire to multiple spheres at equal lengths along the length of the initial wire. Similar results have been seen in the literature for Au and Cu nanowires [14–16]. As the temperature of the substrate and the nanowire network increases due to Joule heating, the atomic diffusion in the nanowire also increases. Since the nanowire is not the lowest energy structure for the
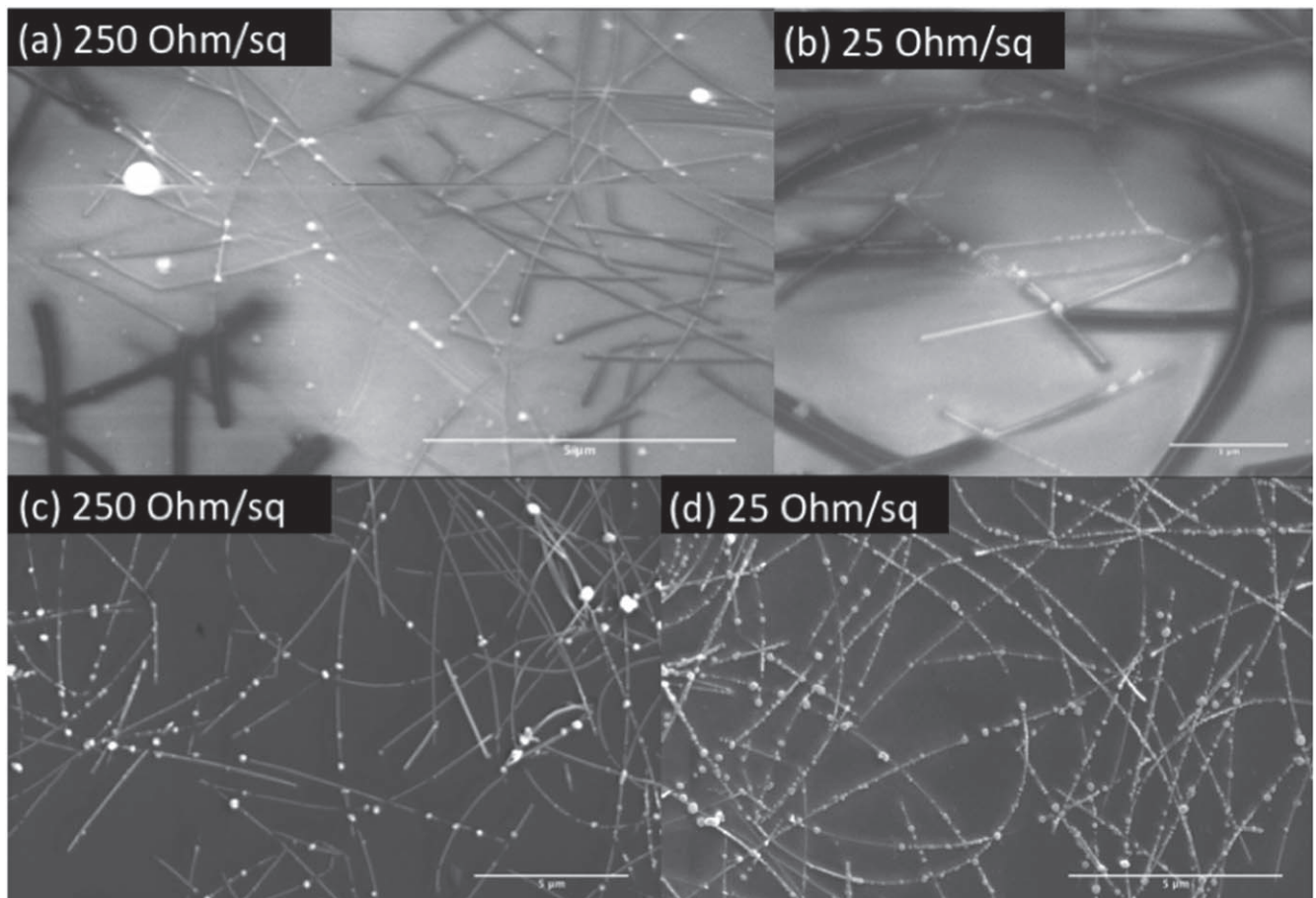
Figure 2. SEM micrographs of failed of nanowire films. (a) and (c) are the failure of a 250 Ohm/sq film, where the failure is initiated at the junctions. (b) and (d) are from a 25 Ohm/sq film where the nanowire network is heated as a whole, resulting in melting of the whole length of the wire.

material, the kinetic limitations to reconstruction can be overcome. As before, not the whole length of the nanowires breaks up, because when the nanowire breaks, current stops passing through it, which in results hinders further heating.

Both types of failures can be seen in samples that have a sheet resistance of $250 \, \Omega/\text{sq}$ and below. The first type of failure, which we suggest is occurring at junctions between nanowires where the contact resistance between nanowires has been estimated to be in the 1.5–$2.5 \, \text{K}\Omega$ region [17]. In comparison, the resistance of a single nanowire with dimensions similar to the ones we are using, has been reported of having a resistance of $223 \, \Omega$ [4]. The contact resistance dominates over the nanowire resistance because it is an order of magnitude higher, resulting in higher heating. The second type of failure occurs due to the more widespread heating of the network (and substrate) as a whole. Such failure occurs in samples with lower sheet resistances and hence higher densities of nanowires. As a consequence, there will be significantly more junctions between nanowires present and multiple layers of nanowires. Due to the increased number of junctions the likelihood of junctions being in proximity to each other is higher. So, the heating of the wires is more significant. Furthermore, since there are multiple layers of wires, the heat acquired is harder to dissipate. This may be happening because the bottom layers dissipate heat readily

through the glass substrate with which they are in more intimate contact with, which is more thermally conductive than the air that surrounds them. This has been observed previously, where the laser ablation threshold of multi-layered nanowire films was found to be disproportionately lower than that of single layer films [18].

The failure power per nanowire for a range of films with different coating sheet resistances was measured for three sets of nanowire widths (figure 4 left). The widths of the nanowires were measured by atomic force microscopy. The number of nanowires per unit area, was extrapolated from multiple samples and measuring areas. The failure power per nanowire was then calculated by dividing the power that the samples failed at during tests by the number of nanowires calculated. The first observation from this data is that higher density nanowire networks (lower sheet resistances) fail at lower power per nanowire (figure 4 left). It is suggested that this is due to the lack of heat dissipation from the nanowires that are not touching the substrate. This is further supporting the findings from the SEM micrographs. Additionally, it was observed that nanowires of different diameters fail at different power densities, with thicker nanowires withstanding a higher current through them allowing them to reach higher temperatures. This has been seen in nanoparticles as well, where
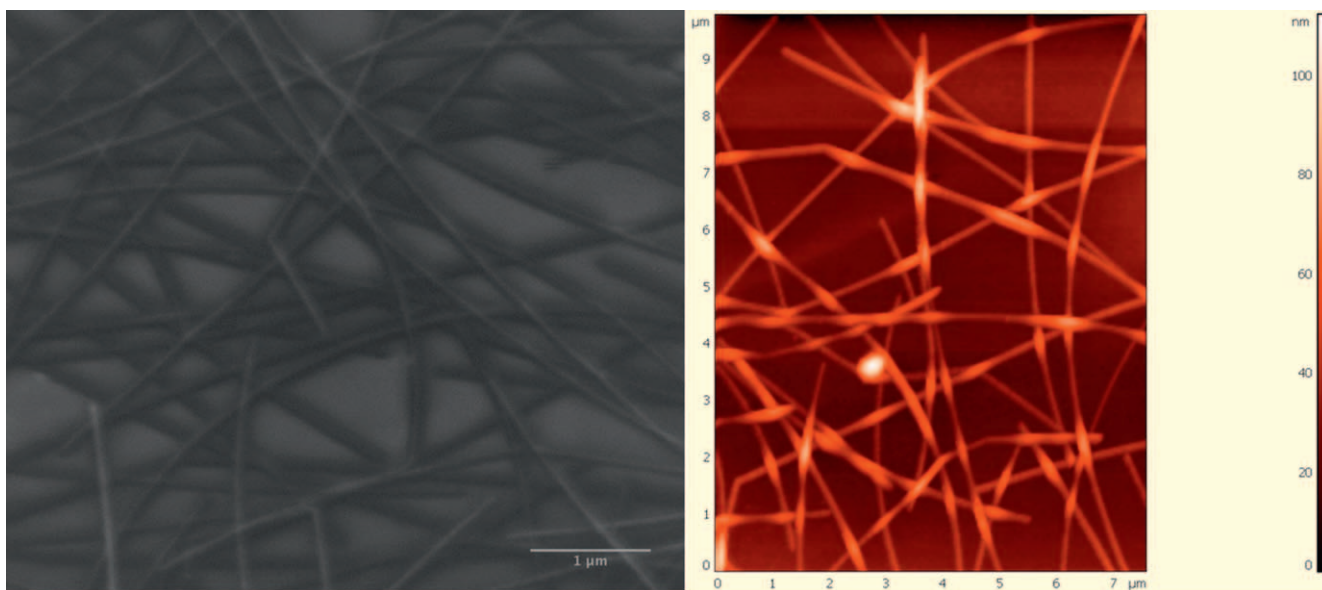
Figure 3. (Left) SEM micrograph showing a pristine nanowire network. The nanowire coating is random and uniform and there are no nanoparticles or other impurities present. (right) AFM image showing a heated nanowire network. The junctions are not fused together, since the height at the junction is higher and a multiple of the nanowire thickness.

the melting point of the particles increases with increasing diameter. The 15 nm nanowires are close to the theoretical stability limit, hence they will fail at lower temperatures [14]. The improvement we see on the sheet resistance of the network is due to the improvement of the contact resistance of the wires, either by welding or by removing the surfactants from the surface of the wires. This explains as well, the vast difference between the two different nanowires manufacturers, the one that is making the 15 and 30 nm wires and the one of the 40 nm. It is believed that the surfactants and the length distribution of the later are increasing the overall contact resistance of the network, resulting at higher temperatures at the junctions during the Joule heating and therefore failure at lower power per nanowire. In order to examine if the contact resistance is a more significant factor in the overall resistance for the 40 nm wide wires the change in resistance was studied after heating the nanowire networks in a laboratory oven at 180 °C for 30 min; shorter times provided a smaller improvement and longer times had no effect. It has been shown in literature that the sheet resistance of nanowire networks can be improved by removing the polymer surfactant layer [19–21]. Since welding of the wires is not observed (figure 3 right), we are confident that the improvement of the sheet resistance of the networks is a result of heating, since the surfactant coating has a melting point of 150 °C. Since the surfactant is between the nanowires at junctions and it is not conductive, the contact resistance is improved by melting the polymer. By heating the nanowires, an improvement of 20% on average and up to 60%, for the 40 nm wires, was observed. A similar improvement was observed for the 30 nm width nanowires. The 15 nm width wires failed at any temperature above 120 °C and they showed no improvement at temperatures below that, again confirming the lower stability of narrower nanowires.

In figure 4 right, it can be seen that the failure current density of the wires shows a similar trend. Furthermore, in this figure, it can be seen that the levels of failure current density are three orders of magnitude lower than that reported in literature [4]. In literature the values are ranging from 20 up to 260 MA cm^{-2}, but these values are for single nanowires. This highlights the importance of contact resistance in understanding failure of nanowire networks, particularly for high density networks where heat dissipation is expected to be poorer, because a higher percentage of nanowires are not in contact with the substrate and only have air to dissipate the heat through, which is a worse heat conductor. This has been observed in literature for the laser ablation of nanowires, where denser networks require a lower laser fluence in order to be removed [18]. Cheng *et al* have shown that the thermal conductivity of the nanowire network improves with higher densities of wires [22]. Even though that is the case, the lack of a 'heat sink' material to dissipate the heat through, results in higher temperature and resulting failure. The only way to achieve similar levels, would be by eliminating contact resistance.

Like all conductors, Ag nanowires produce heat when current passes through them, due to Joule heating. This is also known as ohmic heating and the amount of heat released (Q) is proportional to the square of the current and the time (t) as can be seen from the Joule–Lenz Law relationship below (equation (2.1)):

$$Q \propto I^2 Rt. \tag{2.1}$$

Due to the higher resistance at the junctions of wires, which is a result of the contact resistance at that region, the heating effect is higher there. In literature the contact resistance has been estimated to be in the 1.5–2.5 KΩ region [17]. At the same time the resistance of a single nanowire with dimensions similar to the ones we are using, has been reported of having a resistance of 223 Ω [4].
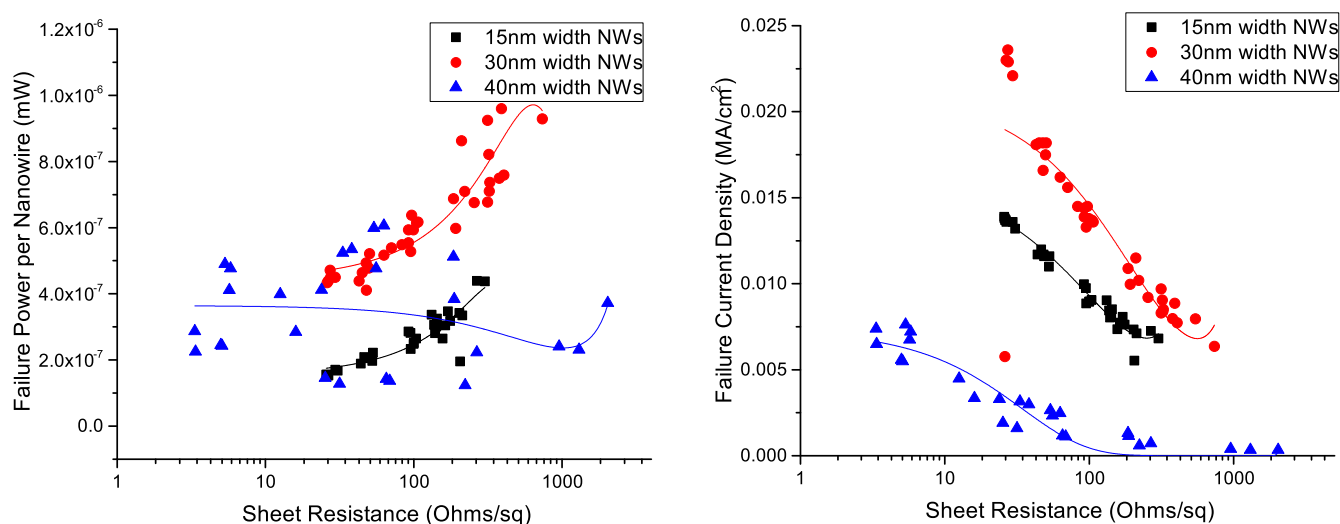
Figure 4. The failure power per nanowire of three different width nanowires (left) and the failure current density (right). It can be seen that with increasing nanowire width, the robustness of the resulting network is increasing, between the 15 and 30 nm nanowires, which are from the same manufacturer., while the 40 nm wires are from a different supplier and have different properties, which is believed to be due to the different surfactants and length distributions.

In order to support our findings regarding the failure mechanism, simulations of nanowire networks consisting of three nanowires were conducted using the finite element multi-physics package COMSOL. Here, both the joule heating and thermal diffusion can be simulated for arbitrary nanowire dimension. Literature values for the properties of the nanowires and their contacts were used [17] and built-in parameters for the glass substrate and the air around the sample were used. For these simulations the assumption that perfect thermal contact between the nanowires and substrate is taken. Having less than perfect contact between the wires and the substrate would result in higher temperatures, due to worse thermal conductivity. The contact resistance was simulated using a spacer. The spacer was modeled having the thermal conductivity of silver, but with a resistance higher than the nanowires, to simulate contact resistance [17]. While this is unlikely to be realistic for actual systems where surface roughness will diminish thermal conductivity, the value of this simulation is in evaluation the potential scale of the effect of contact versus non-contract. Two different scenarios; all the nanowires touching the substrate, which simulates a sparse network and with the nanowire suspended from other nanowires and not touching the glass substrate, which simulates a dense network, where the top nanowires are not touching the substrate, were simulated. The junction between the nanowires was simulated using a very thin layer of high electrical resistance material placed between the contacting geometries. In figure 5 the heating of the nanowires in these two scenarios can be seen. It is clear that in both scenarios, the heating is most significant at the junctions, where the contact resistance is higher. It is also clear that the suspended nanowire heats up much more and along its full length. This correlates with the SEM micrographs of failed nanowire networks, where for denser films melting over the whole length of the nanowire is observed. Furthermore, the temperature of the suspended wire is significantly higher (257 °C),

which would suggest a premature failure. The non-suspended wire is using the substrate as a heatsink, to dissipate its heat through.

In order to improve the robustness of the nanowire film a way of dissipating the heat is needed. A nanowire/poly(3,4-ethylenedioxythiophene) polystyrene sulfonate (PEDOT:PSS) hybrid, was evaluated as a potential way to manage heat dissipation. PEDOT:PSS is another transparent conductive material. However, here the PEDOT:PSS film will act as a heat dissipation layer. To do this nanowire samples of various sheet resistances were spray deposited and then spray with PEDOT:PSS on top. The nanowires chosen were the 40 nm nanowires, which showed the worst performance before. The sheet resistance of the sprayed PEDOT:PSS film was 500 Ω/sq.

The PEDOT improved the nanowire sheet resistance by an average of 34.5%, by depositing a 500 Ω/sq PEDOT film. The response of the hybrid samples was different to that of samples that contained only nanowires. Figure 6 right, shows a micrograph of such film. The nanowires can be seen to be melted through their whole length leaving behind silver blobs or large nanoparticles, similarly to very dense films. This type of failure is observed in all the samples irrespective of the density of the film. We believe that the PEDOT:PSS film was affected as well, as extreme failure was also accompanied by emission of a smoky vapor from the samples. However, in many cases the samples did not fail completely, and some residual conductivity was still observed. In literature the removal of PSS from PEDOT:PSS has shown an improvement of the conductivity of these polymer films. The combination of PEDOT:PSS with the silver nanoparticles maintained the film conductive for longer. In the left part of figure 6 the failure power per nanowire of the PEDOT hybrid film and the pristine nanowire film are compared. The hybrid sample can withstand a higher power especially at higher sheet resistances. This shows us that the PEDOT film is
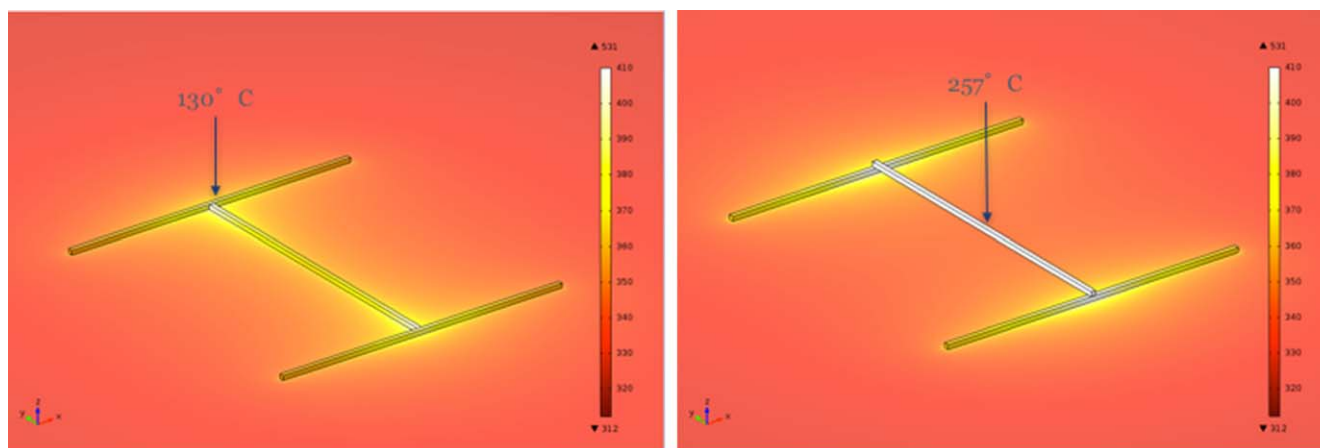
Figure 5. COMSOL simulations of the heating of the nanowires in a network. The left image is showing the heating of a sparse network, where all the nanowires are in contact with the substrate. In this case the junctions are the hottest point, reaching temperatures of 130 °C after 1 s. The right image shows the heating of a dense network, where not all nanowires are in contact with the substrate. In this case the suspended nanowires are heating up in the whole length at higher temperatures than in the first case, reaching 257 °C in 1 s.
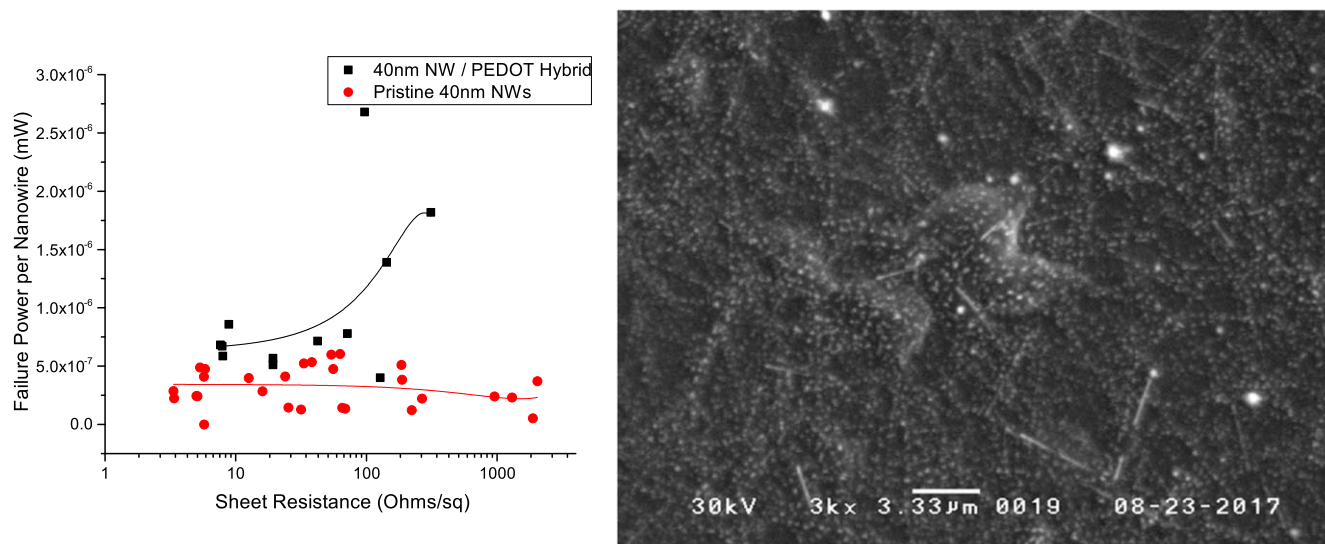

Figure 6. In the left part of the figure, the failure power per nanowire of a pristine nanowire film is compared with a film of the same type of nanowires with a PEDOT film spray deposited on top. It can be seen that the nanowires can withstand a higher power, due to the PEDOT film dissipating the heat. In the right image an SEM micrograph of the failure of a Ag NW/PEDOT hybrid film is presented. The failure is similar of that of a dense film, because the heat is spread through the PEDOT to the whole nanowire network.

aiding in the heat dissipation and also, by creating more conductive paths for the current to flow through. We know that the heat is dissipated from the junctions because of the type of failures of the nanowires we observed. The failure of these films is similar to dense networks. Hence, the PEDOT film was absorbing the heat up to the point that the temperature melted the nanowires.

resistance and find a way to dissipate the heat produced that result in failures. When the contact resistance is eliminated, networks with lower sheet resistance, but with the same number of nanowires and hence optical transmission, can be achieved. This can result in current densities closer to those reported in literature for single wires, which range from 18 up to 260 MA cm^{-2} [4].

4. Conclusion

Based on the measurements performed here, the failure mechanisms for large networks of AgNWs under direct current load have been identified as junctional failure and whole-wire failure with the proportion of each depending on the NW film architecture. It is suggested that the main focus to improve the failure current density is to reduce the contact

Acknowledgments

ORCID iDs

D Fantanas ● https://orcid.org/0000-0002-4068-123X

References

[1] Burgess L 2007 *Indium Demand: Our Indelible Interest in Indium* (Baltimore, MD: Wealth Daily)

[2] Langley D, Giusti G, Mayousse C, Celle C, Bellet D and Simonato J-P 2013 Flexible transparent conductive materials based on silver nanowire networks: a review *Nanotechnology* **24** 45

[3] Tsuchiya K, Li Y and Saka M 2014 Consistent melting behavior induced by Joule heating between Ag microwire and nanowire meshes *Nanoscale Res. Lett.* **9** 8

[4] Wiley B J, Wang Z H, Wei J, Yin Y D, Cobden D H and Xia Y N 2006 Synthesis and electrical characterization of silver nanobeams *Nano Lett.* **6** 2273–8

[5] Kaspers M R, Bernhart A M, Heringdorf F J M Z, Dumpich G and Moeller R 2009 Electromigration and potentiometry measurements of single-crystalline Ag nanowires under UHV conditions *J. Phys.: Condens. Matter* **21** 26

[6] Khaligh H H and Goldthorpe I A 2013 Failure of silver nanowire transparent electrodes under current flow *Nanoscale Res. Lett.* **8** 235

[7] Hsiao S-T, Tien H-W, Liao W-H, Wang Y-S, Li S-M, MMa C-C, Yu Y-H and Chuang W-P 2014 A highly electrically conductive graphene-silver nanowire hybrid nanomaterial for transparent conductive films *J. Mater. Chem. C* **2** 7284–91

[8] Lee J, Lee P, Lee H, Lee D, Lee S S and Ko S H 2012 Very long Ag nanowire synthesis and its application in a highly transparent, conductive and flexible metal electrode touch panel *Nanoscale* **4** 6408–14

[9] Mayousse C, Celle C, Fraczkiewicz A and Simonato J P 2015 Stability of silver nanowire based electrodes under environmental and electrical stresses *Nanoscale* **7** 2107–15

[10] Liu X, Zhu J, Jin C, Peng L-M, Tang D and Cheng H 2008 *In situ* electrical measurements of polytypic silver nanowires *Nanotechnology* **19** 8

[11] Sun Y G, Mayers B and Xia Y N 2003 Transformation of silver nanospheres into nanobelts and triangular nanoplates through a thermal process *Nano Lett.* **3** 675–9

[12] Sun Y G, Mayers B, Herricks T and Xia Y N 2003 Polyol synthesis of uniform silver nanowires: a plausible growth mechanism and the supporting evidence *Nano Lett.* **3** 955–60

[13] Khaligh H H, Xu L, Khosropour A, Madeira A, Romano M, Pradere C, Treguer-Delapierre M, Servant L, Pope M A and Goldthorpe I A 2017 The Joule heating problem in silver nanowire transparent electrodes *Nanotechnology* **28** 42

[14] Bid A, Bora A and Raychaudhuri A K 2005 *SPIE, Proc. Society of Photo-Optical Instrumentation Engineers* vol 5843 *(Austin, TX, 24–25 May)* (SPIE) pp 147–54

[15] Karim S, Toimil-Molares M E, Balogh A G, Ensinger W, Cornelius T W, Khan E U and Neumann R 2006 Morphological evolution of Au nanowires controlled by Rayleigh instability *Nanotechnology* **17** 5954–9

[16] Toimil-Molares M E, Balogh A G, Cornelius T W, Neumann R and Trautmann C 2004 Fragmentation of nanowires driven by Rayleigh instability *Appl. Phys. Lett.* **85** 5337–9

[17] Mutiso R M, Sherrott M C, Rathmell A R, Wiley B J and Winey K I 2013 Integrating simulations and experiments to predict sheet resistance and optical transmittance in nanowire films for transparent conductors *ACS Nano* **7** 7654–63

[18] Henley S J, Cann M, Jurewicz I, Dalton A and Milne D 2014 Laser patterning of transparent conductive metal nanowire coatings: simulation and experiment *Nanoscale* **6** 946–52

[19] Lee J, Lee I, Kim T S and Lee J Y 2013 Efficient welding of silver nanowire networks without post-processing *Small* **9** 2887–94

[20] Lee J Y, Connor S T, Cui Y and Peumans P 2008 Solution-processed metal nanowire mesh transparent electrodes *Nano Lett.* **8** 689–92

[21] Tokuno T, Nogi M, Karakawa M, Jiu J T, Nge T T, Aso Y and Suganuma K 2011 Fabrication of silver nanowire transparent electrodes at room temperature *Nano Res.* **4** 1215–22

[22] Cheng Z, Han M, Yuan P Y, Xu S, Cola B A and Wang X W 2016 Strongly anisotropic thermal and electrical conductivities of a self-assembled silver nanowire network *RSC Adv.* **6** 90674–81